The attached reverse and detached forward cascades in wall-turbulent flows

The attached reverse and detached forward cascades in wall-turbulent flows

Andrea Cimarelli[1], Elisabetta De Angelis[1], Alessandro Talamelli[1], Carlo Massimo Casciola[2] and Javier Jiménez[3]

[1]Dipartimento di Ingegneria Industriale, Università di Bologna, 47121 Forlì, Italy
[2]Dipartimento di Ingegneria Meccanica e Aerospaziale, Università di Roma La Sapienza, 00185 Roma, Italy
[3]School of Aeronautics, Universidad Politécnica de Madrid, 28040 Madrid, Spain

E-mail: `andrea.cimarelli2@unibo.it`

Abstract. The present work describes the multidimensional behaviour of wall-bounded turbulence in the space of cross-scales (spanwise and wall-normal) and distances from the wall. This approach allows us to understand the cascade mechanisms by which scale-energy is transmitted scale-by-scale away from the wall, through the overlap layer, and into the bulk flow. Two distinct cascades are identified involving the attached and detached scales of motion, respectively. From the near-wall region, scale-energy is transferred towards the bulk, flowing through the attached scales of motion, while among the detached scales it converges towards small scales, ascending again to the channel centre. It is then argued that the attached scales of wall-bounded turbulence are involved in a reverse cascade process that starts from the wall and ends in the bulk flow. On the other hand, the detached scales belong to a direct forward cascade process towards dissipation. Hence, at a given distance from the wall the attached motion is fed by smaller attached scales located closer to the wall. In turn this attached motion is responsible for creating the scale-energy that sustains larger attached scales farther from the wall and smaller detached scales that are responsible for connecting the scale-energy at large scales to the dissipation at small scales through a forward cascade.

1. Introduction

The presence of a mean velocity gradient makes wall-turbulent flows anisotropic and provides a continuous source of kinetic energy. Shear flows do not need large-scale forcing to maintain turbulence in a statistically steady state. The mean shear makes wall flows also intrinsically inhomogeneous. Thanks to inhomogeneity, wall-bounded flows have been classically studied by dividing the flow domain into well-defined regions. The local production of turbulent fluctuations exceeds the rate of dissipation near the wall, in the so-called buffer layer, while the opposite occurs at the wall and in the bulk of the flow. The turbulent fluctuations in these regions are then fed in part by a spatial flux of energy emerging from the energy excess in the buffer layer. But actually, a third layer exists, forming an intermediate region between the energy source region near the wall and the energy sink region in the bulk flow, the so-called overlap layer. In the classical view, the production of turbulent fluctuations in this region approximately balances dissipation (equilibrium layer) and, hence, the flux of energy from the wall to the bulk is approximately constant. Energy is neither received from nor released to the spatial flux.

Turbulence in this layer is self-similar, and the distance to the wall acts as a similarity scale, leading to a logarithmic velocity profile [1].

The description in physical space alone is, however, insufficient to capture the real dynamics of wall-bounded turbulence, and traditionally it is complemented by a parallel view based on the decomposition of the field into a hierarchy of scales of motion. In fact, every turbulent flow is characterized by interactions of fluctuations of different sizes and intensities and, at sufficiently high Reynolds number, a universal state governed by an energy cascade from large to small scales is expected to take place [2]. Hence, in wall-bounded flows a classical cascade across different eddy sizes is superimposed on a spatial energy transfer.

Then, a fundamental issue in wall-bounded flows is the understanding of the cascade mechanism by which energy is transmitted scale-by-scale away from the wall, through the overlap layer, and into the bulk flow. Recent works dealt with this problem by means of numerical data of turbulent channel flows. In particular, Ref. [3], by using the balance equation for the second-order structure function, the so-called generalized Kolmogorov equation, studied how turbulent energy is transferred from the production to the dissipation regions of the compound space of scales and wall-distances, (r, Y_c). More recently, this work has been extended in [4, 5], accounting also for the anisotropic features of the space of wall-parallel scales (r_x, r_z). In these works, the analysis of the augmented space, (r_x, r_z, Y_c), revealed that the long and wide fluctuating structures are fed by a small-scale region of energy source near the wall through a reverse energy transfer. The need to adopt a multidimensional approach is also shown to be fundamental for the understanding of the interrelated processes governing wall-turbulence. However, there are a number of open issues to be addressed. The first one concerns the behaviour of energy in the complete four-dimensional space, i.e including the wall-normal scales, r_y. Indeed, the analysis of r_y allows us to study directly the behaviour of the so-called attached and detached eddies, i.e. those scales of motion that are of the same order and smaller, respectively, than the wall-distance considered.

The study of the dynamics related to attached and detached scales is fundamental for the comprehension of the high-Reynolds-number asymptotic state of wall turbulence. It is argued that the overlap layer dominates at sufficiently high Reynolds numbers by contributing to the bulk production more than the near-wall region [6]. In turn, the overlap layer is thought to be populated by a hierarchy of attached eddies that are then conjectured to govern the high-Reynolds-number state of wall-turbulence [7, 8].

From the similarity hypothesis and from momentum conservation, which implies that the shear stress, $\tau = -\langle uv \rangle$, is constant and equals u_τ^2 near the wall, the overlap layer should be traversed by a constant spatial flux, $\phi/u_\tau^3 = const$, and, hence, production should balance dissipation. Here, $u_\tau = \sqrt{\tau_w/\rho}$ is the friction velocity, with τ_w the average shear stress at the wall, and ρ the constant density of the fluid. Because the energy-containing scales are small near the wall, while those further away from the wall are large (see figure 1 to have an approximate idea of the topology of the flow field), this transfer of energy is conjectured to be an example of inverse cascade [9, 10]. Energy is transferred to smaller scales at any given location, and to larger ones away from the wall. Since the smallest scales of the flow are thought to be isotropic and to carry no mean shear stress, the larger ones are those responsible for the momentum cascade. Because of the different type of fluxes involved, this cascade process is different from the Kolmogorov one. For scales larger than the wall-distance, the spectrum depends on the momentum flux u_τ^2, and on the wavenumber k, and is independent of the wall-distance. Hence, the k^{-1}-law for the spectrum is obtained, $E(k) \sim u_\tau^2 k^{-1}$ [11]. On the other hand, the smaller scales do not interact with the wall and break down into smaller eddies, following a classical Kolmogorov cascade. This attached/detached eddy picture of energy transfer was first proposed in [1], but still has to be assessed. In this context, the aim of the present work is to verify these theories and to assess the similarities, differences, and interactions between those two cascades.
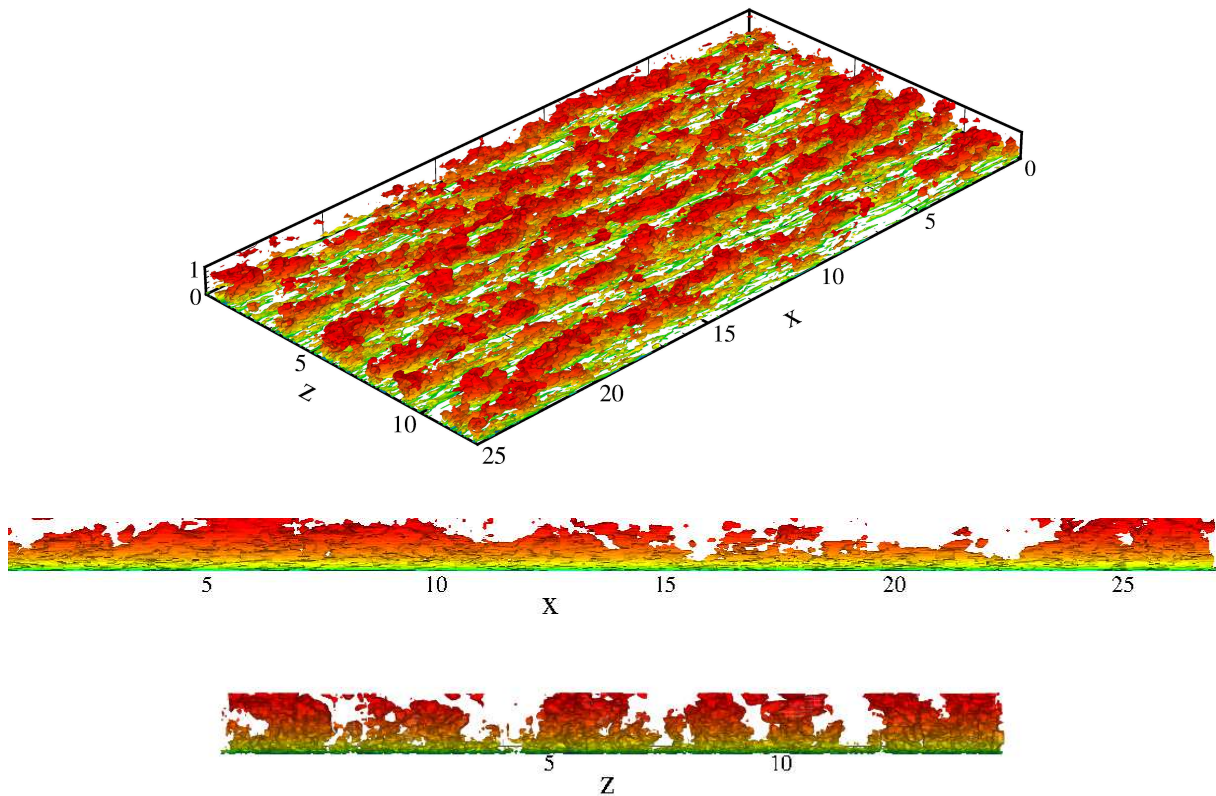
Figure 1. Direct numerical simulation of a turbulent channel flow at $Re_\tau = 550$ [14]. Isosurfaces of a negative value of the streamwise velocity fluctuations, with colours encoding wall distance. Perspective, lateral and frontal views are shown from top to bottom. The streamwise, wall-normal and spanwise directions, (x, y, z), are normalized by the channel half-height, h.

2. The compound (r_y, r_z, Y_c)-space

Energy transfer, production and dissipation are the relevant processes in turbulence. They take place in various ranges of scales and, for inhomogeneous flows, change in different flow regions. As a consequence, a full understanding of these interacting phenomena requires a detailed description of the processes occurring simultaneously in physical and scale space. To this aim, we study the second-order structure function $\langle \delta u^2 \rangle$, where $\delta u^2 = \delta u_i \delta u_i$, $\delta u_i = u_i(X_s + r_s/2) - u_i(X_s - r_s/2)$ is the fluctuating velocity increment, and angle brackets denote ensemble averaging. It is a function of the separation vector r_s and of the mid-point X_s, allowing to describe the scale-dependent mechanisms in the presence of inhomogeneity. Hereafter we will refer to the concept of scale-energy while speaking about the second-order structure function. Although this quantity has the dimensions of kinetic energy, its interpretation in terms of kinetic energy of turbulent structures of a given size is not strict. Indeed, while being strictly related to the energy spectrum, it is not an intensive quantity, i.e. the integral in the space of scales of $\langle \delta u^2 \rangle$ has no meaning. It should be stressed however that, despite some difficulties in its interpretation (see [12] and its appendix), the scale-energy is the natural tool for the statistical analysis of general turbulent flows that lack a classical spectral decomposition due to violation of spatial homogeneity. As it will be shown below, it allows addressing the multidimensional cascade mechanisms and in particular the related attached/detached features.

The governing equation of $\langle \delta u^2 \rangle$ in wall flows is the generalized Kolmogorov equation [13, 3],
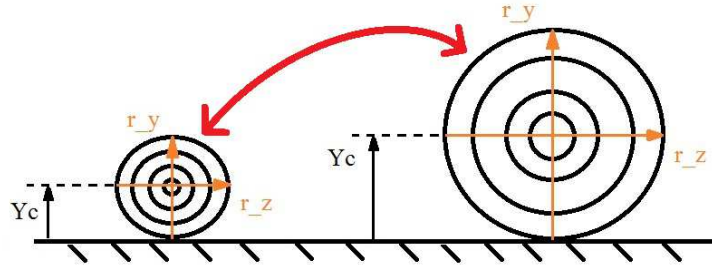
Figure 2. Idealized picture of the (r_y, r_z, Y_c)-space.

which for a turbulent channel flow with longitudinal mean velocity $U(y)$ reads

$$\frac{\partial \langle \delta u^2 \delta u_i \rangle}{\partial r_i} + \frac{\partial \langle \delta u^2 \delta U \rangle}{\partial r_x} + 2\langle \delta u \delta v \rangle \left(\frac{dU}{dy}\right)^* + 2\langle \delta u v^* \rangle \, \delta\!\left(\frac{dU}{dy}\right) + \frac{\partial \langle v^* \delta u^2 \rangle}{\partial Y_c} =$$

$$-4\langle \epsilon^* \rangle + 2\nu \frac{\partial^2 \langle \delta u^2 \rangle}{\partial r_i \partial r_i} - \frac{2}{\rho} \frac{\partial \langle \delta p \delta v \rangle}{\partial Y_c} + \frac{\nu}{2} \frac{\partial^2 \langle \delta u^2 \rangle}{\partial Y_c^2} \tag{1}$$

where the asterisk denotes the arithmetic average of a variable at the points $X_s \pm r_s/2$, $Y_c = X_2$ is the wall-normal coordinate of the mid-point, $v = u_2$ is the wall-normal velocity, ν is kinematic viscosity, and $\epsilon = \nu(\partial u_i / \partial x_j)(\partial u_i / \partial x_j)$ is the pseudo-dissipation. As shown in [4, 5], it is useful to recast equation (1) in terms of a four-dimensional vector field, $\boldsymbol{\Phi} = (\Phi_{r_x}, \Phi_{r_y}, \Phi_{r_z}, \Phi_c)$, hereafter called the scale-energy hyper-flux defined in a four dimensional space (r_x, r_y, r_z, Y_c),

$$\nabla_4 \cdot \boldsymbol{\Phi}(\mathbf{r}, Y_c) = \xi(\mathbf{r}, Y_c), \tag{2}$$

where ∇_4 is the four-dimensional gradient and $\xi = -2\langle \delta u \delta v \rangle (dU/dy)^* - 2\langle \delta u v^* \rangle \, \delta(dU/dy) - 4\langle \epsilon^* \rangle$ is the scale-energy source/sink. The flux in the three-dimensional space of scales is $\boldsymbol{\Phi}_r = (\Phi_{r_x}, \Phi_{r_y}, \Phi_{r_z}) = \langle \delta u^2 \delta \mathbf{u} \rangle + \langle \delta u^2 \delta U \rangle \hat{\mathbf{e}}_x - 2\nu \nabla_r \langle \delta u^2 \rangle)$, where $\hat{\mathbf{e}}_x$ is the unit vector in the mean flow direction x. In addition to the flux in the space of scales, the generalized Kolmogorov equation features the spatial flux $\Phi_c = \langle v^* \delta u^2 \rangle + 2\langle \delta p \delta v \rangle / \rho - \nu/2 \partial \langle \delta u^2 \rangle / \partial Y_c$. As mentioned above, equation (2) has been analysed in [4, 5] in the hyper-plane $r_y = 0$ of the four-dimensional space. This approach allowed to identify the reverse energy transfer as the crucial mechanisms characterizing wall turbulence, responsible for the formation of the commonly observed very long and wide velocity fluctuations. Here, in order to focus on the conjectured dual cascades involving attached/detached scales, the analysis will be performed in the hyper-plane $r_x = 0$, i.e. in the (r_y, r_z, Y_c)-space. Indeed, the space of the cross-scales most clearly allows to detect the attached/detached feature of the statistics related to scales of motion whose vertical length, r_y, is equal-to/smaller-than twice the wall-distance of their centre, Y_c (see figure 2). The idealized picture of figure 2 sketches also how equation (2) is used to detect the scale-energy transfer in the space of scales, i.e. along the orange (r_y, r_z)-axis, and the transport in physical space, i.e. along the Y_c-axis (red arrow).

Given the definition of velocity increments, the r_y direction is limited by the presence of the wall. In particular, for a given wall-distance Y_c, the space of wall-normal scales extends from zero to twice the distance from the wall, $r_y \in [0, 2Y_c]$. Actually, negative increments, i.e. $r_y \in [-2Y_c, 2Y_c]$, are not considered here since the symmetry of the flow is such that the transformation $\mathbf{r} \to -\mathbf{r}$, $\widetilde{Y}_c = const$ leads to $\boldsymbol{\Phi}_r \to -\boldsymbol{\Phi}_r$ and $\Phi_c \to \Phi_c$. This transformation leaves quantities like δu^2 and v^* statistically invariant while reversing the sign of vectors like δu_i
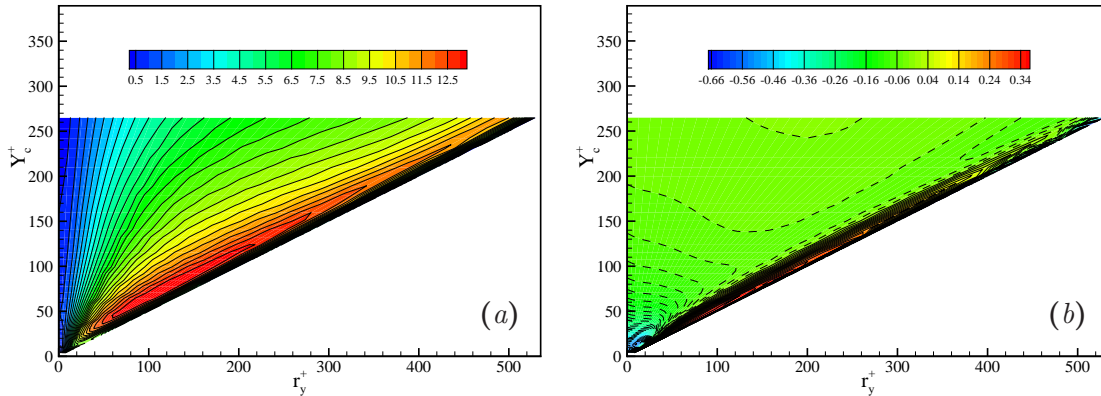
Figure 3. Section of the reduced space (r_y, r_z, Y_c) in the $r_z = 0$-plane. The isocontours show the behaviour of scale-energy, $\langle \delta u^2 \rangle^+$, (left) and of the source/sink term, ξ^+, (right). Solid and dashed lines denote positive and negative values, respectively.

and ∇_r. On the boundary $r_y = 2Y_c$ the scale-energy equals the single-point turbulent kinetic energy,

$$\langle \delta u^2 \rangle = \langle u_{ii}^2 \rangle \big|_{y=2Y_c} \ ,$$

where $u_{ii}^2 = u^2 + v^2 + w^2$, while the fluxes with a component normal to the boundary take the form

$$\Phi_{r_y} = \langle u_{ii}^2 v \rangle \big|_{y=2Y_c} - \nu \frac{\partial \langle u_{ii}^2 \rangle}{\partial y}\bigg|_{y=2Y_c}$$

$$\Phi_c = \frac{1}{2}\langle u_{ii}^2 v \rangle \big|_{y=2Y_c} - \frac{1}{2}\nu \frac{\partial \langle u_{ii}^2 \rangle}{\partial y}\bigg|_{y=2Y_c} + \frac{2}{\rho}\langle \delta p(v|_{y=2Y_c}) \rangle \ .$$

From the above equations we argue that the fluxes could be aligned to the boundary ($r_y = 2Y_c, Y_c$) only when the pressure term for the spatial flux is negligible, since in this case we would have $\Phi_{r_y} = 2\Phi_c$. As will be shown in what follows, the role of the ($r_y = 2Y_c$)-plane is very important, since the wall-normal scales close to this plane represent the attached features of the flow and, hence, that is the layer where the reverse cascade process and the other paradigms mentioned in the introduction should occur. Smaller wall-normal scales represent instead the detached features of the flow, where an overall forward cascade is expected to take place.

The data used for the present analysis come from a channel-flow DNS at $Re_\tau = u_\tau h / \nu = 550$, where h is the channel half-height. Throughout the paper, inner variables will be used and denoted with $+$ as superscript, implying normalization of lengths with the friction scale ν / u_τ and velocities with u_τ. The simulations have been carried out with a pseudo-spectral code. The computational domain is $8\pi h \times 2h \times 4\pi h$ with $1024 \times 257 \times 1024$ grid points, respectively, corresponding to a resolution in the homogeneous directions of $\Delta x^+ = 13.5$ and $\Delta z^+ = 6.7$ [14].

3. Results

Let us first analyse how the scale-energy and the scale-energy source are distributed as functions of the wall-normal separation, r_y, for different distances from the wall, Y_c. As shown in figure 3(a), the scale-energy attains a clear maximum that, for each wall-distance, is located near the ($r_y = 2Y_c$)-plane. This is clear statistical evidence of fluctuations occurring on a scale extending down to the wall, in the sense of the attached eddies of Townsend [1]. The wall-normal position
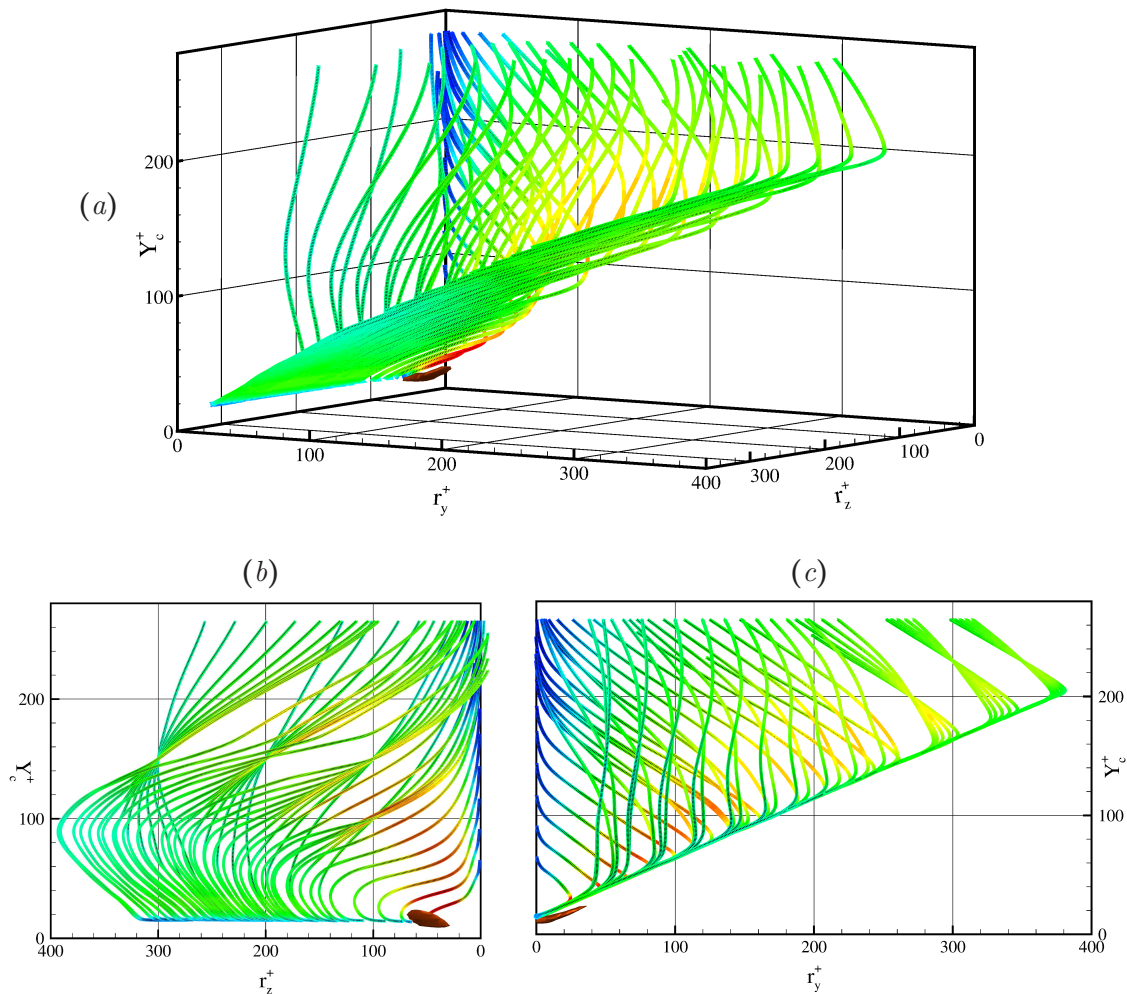
Figure 4. Trajectories of the scale-energy fluxes (colours according to strength) in the (r_y, r_z, Y_c)-space. The red iso-surface shows the maximum for the source term, $\xi^+ = 0.61$.

of the maximum in the scale-energy confirms the relevance of such scales in the putative overlap layer. Namely, these attached scales are not only the most energetic of the $(r_z = 0)$-plane (wall-normal scales, wall-distance) but, as shown in figure 3(b), are also responsible for most of the production of turbulence. Apparently, the source term ξ presents a strong positive peak for scales spanning the distance to the wall, even for Y_c far away from the near-wall production region. This observation is consistent with the conjecture of a second outer turbulent regeneration cycle in the overlap layer [15] involving turbulent fluctuations that scale with the wall-distance [16, 17]. In order to avoid possible misunderstandings, we stress that the source and scale-energy related to the near-wall cycle are not visible in figure 3, which is a section of the (r_y, r_z, Y_c) at $r_z = 0$. Indeed, as it will be shown below and has been discussed already in [4], the near-wall source occurs in a precise range of spanwise scales with $r_z \neq 0$.

Let us now analyse the multidimensional behaviour of scale-energy from production to dissipation in the entire (r_y, r_z, Y_c)-space. As shown by the field lines in figure 4, scale energy emerges from the small scales in the near-wall region and, ascending, feeds larger and taller fluctuations before converging to small dissipative scales. The origin of the fluxes is located in the small scales of the buffer layer, corresponding to the peak of the scale-energy source at $r_y^+ = 7, r_z^+ = 40, Y_c^+ = 13$ (see the red isosurface in figure 4). This is the main source
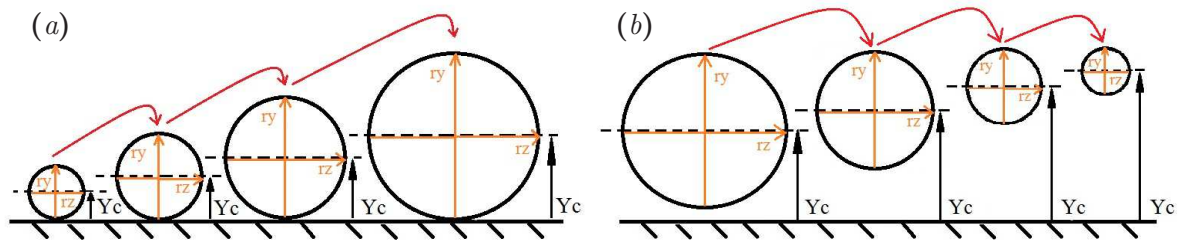
Figure 5. Sketch of the two distinct cascade mechanisms coexisting in wall-flows. (a) The reverse cascade process through attached scales from the wall to the bulk flow. (b) The forward cascade through detached scales up to dissipative scales further away from the wall.

region for the fluxes, while the sinks are distributed continuously with the wall-distance at the smallest scales of motion, close to $r_y = r_z = 0$. From the inspection of the plots it appears that scale-energy flows from the peak of energy source near the wall towards larger fluctuations (larger r_z) following a line of divergence from which the fluxes suddenly depart towards the bulk (see the horizontal envelope at $Y_c^+ \sim 13$ in the bottom-left panel of figure 4). These fluxes become aligned to the ($r_y = 2Y_c$)-plane while ascending (see figure 4c). In turn, this is also a plane of divergence from which the fluxes suddenly depart bending towards smaller scales up to dissipation. Note that the fluxes, while aligned to the ($r_y = 2Y_c$)-plane, move towards larger r_z. In particular, the spanwise scale linearly increases with the wall-distance as half the wall-normal scale, i.e. $r_z \sim r_y/2$. After leaving the ($r_y = 2Y_c$)-plane, the fluxes converge towards smaller r_y and r_z, intercepting narrower and thinner fluctuations. Summarizing, the fluxes leave the line of divergence in the near wall region at $Y_c^+ = 13$ and $r_y^+ = 7$ for different spanwise lengths, denoted as Δz_{nw}^+. The fluxes depart from this line and lie on the ($r_y = 2Y_c$)-plane. In this plane, they intercept wall-normal scales attached to the wall with spanwise scales that linearly increase with wall-distance [18, 19, 20],

$$r_y^+ = 2Y_c^+ \tag{3}$$

$$r_z^+ = \Delta z_{nw}^+ + r_y^+/2 = \Delta z_{nw}^+ + Y_c^+ \sim Y_c^+ \,. \tag{4}$$

It is important to point out that the source term along these paths is always pumping energy, $\xi > 0$. See for example the evident source of scale-energy close to the ($r_y = 2Y_c$)-scales shown in figure 3(b) for $r_z = 0$. As a consequence, the flux is not conserved since a continuous injection of scale-energy occurs along the path. Hence, the attached scales are not simply involved in the reverse cascade process from the wall to the bulk flow. They also play an active role in injecting scale-energy to sustain the reverse cascade mechanism towards attached scales located further away from the wall, and to initialize the forward cascade through detached scales towards dissipation. Summarizing, the above analysis suggests that the turbulent fluctuations attached to the wall govern the overlap layer and provide the scale-energy source contributing to the sustainment of turbulence. Actually, this wall-attached source is the initiator of the Y_c-distributed direct cascade feeding the detached motion down to dissipation and, at the same time, contributes to the attached reverse cascade that feeds turbulence in the bulk of the flow.

It should be noted that in the attached reverse cascade occurring in the ($r_y = 2Y_c$)-plane, all the three components of the flux vector are positive, i.e. scale-energy ascends towards the bulk of the flow moving from small to large scales, as sketched in figure 5(a). In particular, $\Phi_c \sim \Phi_{r_y}/2$, since the fluxes are tangent to the $r_y = 2Y_c$-plane. Furthermore, from figure 4 we also observe that $\Phi_{r_z} \sim \Phi_c$, so that

$$\Phi_{r_z} \sim \Phi_c \sim \Phi_{r_y}/2 > 0 \,,$$
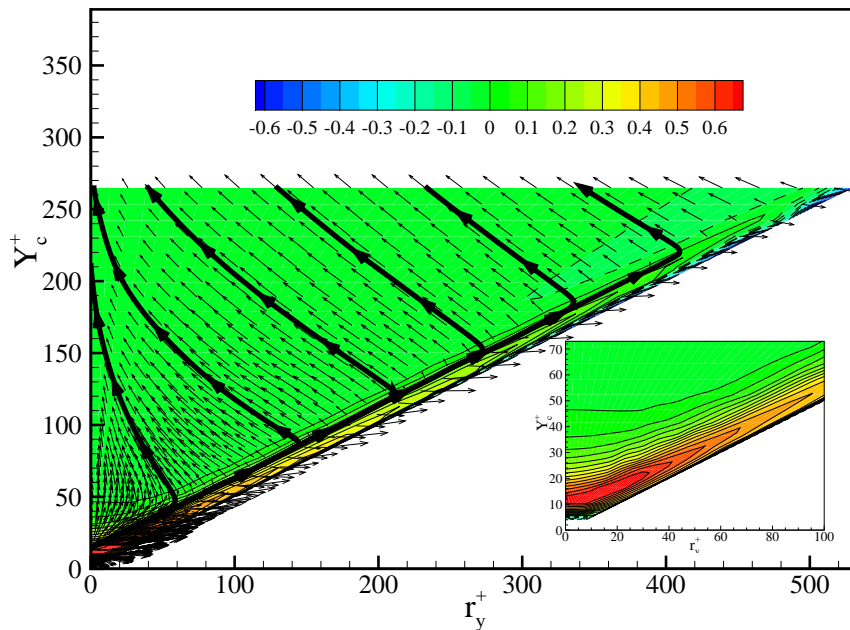
Figure 6. Section of the reduced space (r_y, r_z, Y_c) in the $r_z^+ = 40$-plane. The isocontours show the behaviour of scale-energy source/sink, ξ^+. Solid and dashed lines denote positive and negative values, respectively. Vectors and streamlines show the field of fluxes in this plane. The inset shows a zoom of the source features near the wall.

in agreement with the linear scaling with wall-distance of the spanwise and wall-normal scales in equations (3) and (4). On the contrary, the scale-space fluxes are negative (towards small scales) in the detached direct cascade, while the spatial flux is still positive (towards the bulk of the flow), i.e. a direct cascade ascending to the bulk (see the sketch in figure 5b). By looking at the streamlines in figure 6, we observe that, away from the wall and for large wall-normal scales, the fluxes seemingly approach the inclination

$$\Phi_c \sim -\Phi_{r_y}/2 \ .$$

This behaviour is probably related to a putative inertial range and needs to be verified using data at higher Reynolds numbers. The above relation suggests that the top part of the wall-normal scales intercepted by the direct cascade remains at a constant distance from the wall, i.e., if we define $y_{top} = Y_c + r_y/2$ and $y_{bot} = Y_c - r_y/2$, the direct cascade intercepts smaller and smaller wall-normal scales whose y_{top} is constant, while ascending to the bulk, as sketched in figure 5(b).

It should finally be stressed that the plane of divergence where the attached reverse cascade process occurs is not exactly the $(r_y = 2Y_c)$-plane. As better shown in figure 6, where a cut of the (r_y, r_z, Y_c)-space is shown at the location, $r_z^+ = 40$, of the peak of energy source near the wall, the streamlines of the fluxes and also the isocontours of the source term are aligned and close to the $(r_y = 2Y_c)$-plane but do not lie exactly on it. Furthermore, let us emphasize the quantitative correspondence of the present results with literature. As also shown in [4], the near-wall source mechanisms show a detached feature with the wall-normal scales of the maximum of energy source independent of the wall-distance. See the inset of figure 6, where the isocontours in the neighbourhood of the source maximum near the wall are apparently horizontal. From this detached feature, the source contours start to be aligned to the $(r_y = 2Y_c)$-plane for wall

distances larger than $Y_c^+ \sim 20$. As also pointed out in [7, 8], this wall distance represents the cross-over between the two attached/detached-dominated regions of the flow.

4. Conclusions and final comments

Two cascade mechanisms are found to coexist in wall-turbulence. One involving scales attached to the wall and another characterizing the detached motion. The attached scales are found to be the site of the turbulent production mechanisms driving the overlap layer, and are involved in a reverse cascade process that propagates from the wall to the bulk of the flow. As sketched in figure 5, the attached motion at a given distance Y_c from the wall is fed by a hierarchy of smaller attached scales located closer to the wall. In turn, this attached motion injects scale-energy through a significant scale-energy source, $\xi > 0$, contributing to the propagation of the reverse cascade process towards the bulk, and hence to the sustainment of larger attached scales farther from the wall. The energy source associated to the attached scales is also strong enough to initialize at each distance from the wall a direct forward cascade toward smaller detached scales. This forward cascade represents the Y_c-distributed connection of the production processes in the attached motion with the dissipation at the smallest scales. As sketched in figure 5, this cascade is also superimposed on a spatial flux. At a given distance from the wall a detached scale is intercepted by a flux originating from a hierarchy of larger detached scales located closer to the wall (smaller Y_c), and so on. It is important to point out another peculiar difference between the two cascades here described. The reverse cascade process starts from the wall, is refilled at each wall-distance, and ends up in the bulk of the flow. The forward cascade originates at each wall-distance from the scale-energy source available at attached scales, and ends up further away from the wall at dissipative scales, i.e. the forward cascade feeds the energy dissipation at the smallest scales of each wall-distance.

Let us finally mention the possible implications of the present results for turbulence modelling. In the context of large-eddy simulation (LES), the possibility to analyse the turbulence mechanisms simultaneously in the compound space of scales and positions allows us to understand the overall behaviour of the resolved field as a function of the filter length, and to identify the physics of the small subgrid scales to be modelled [21, 22]. Here, the use of the (r_y, r_z, Y_c)-space directly connects the present results to wall-turbulence LES with near-wall modelling. Indeed, one of the strategies for high-Reynolds-number LES of wall-bounded flow conceives off-wall boundary conditions applied at a Reynolds-number-independent distance from the wall, thereby solving the LES equations only in the bulk flow; see [23] for a review and the references therein. In this context, the understanding of the dynamics in the overlap layer is very important. Indeed, it supports the transfer of momentum from the bulk flow to the wall across a wide range of scales that should be taken into account in the off-wall boundary conditions. Several theories describe the interaction between the inner and outer layer. Here, the attached scales have been shown to be the site of the scale-energy source mechanisms and to provide the transfer to the bulk turbulence, while detached scales have been shown to belong to a direct cascade process simply linking production to dissipation. In this respect, the off-wall boundary condition applied in [15], which mimics the linear dependence with wall-distance of the length scales, seems to be a very promising approach, since it reproduces the attached motion found to play the most important role for the bulk turbulence.

It is worth emphasizing that, from the present results, small attached eddies created near the wall are not implied to migrate to the bulk region to release their energy there. The fact that the overlap layer is traversed by a flux originating from the wall while being refilled by the local scale-energy source does not necessarily mean that the overlap layer dynamics depends on the production features near the wall. Actually, in analogy to the inertial range of turbulence, it appears that the fluxes and other statistics do not depend on how turbulence is generated near the wall [24]. However, in the same way as the inertial range of turbulence needs a large-scale

production range to initialize the universal cascade process towards smaller scales, the overlap layer needs the near-wall energy excess to initialize the reverse cascade process. Hence, although the near-wall cycle provides the triggering mechanism, the resulting attached reverse cascade in the overlap layer could still remain universal, i.e. independent of the details of the near-wall turbulence generation. As an example, the reverse cascade in the overlap layer should look the same irrespective of the presence of wall roughness.

Acknowledgments

References

[1] Townsend A A 1976 *The Structure of Turbulent Shear Flows*, (Cambridge: Cambridge University Press)
[2] Kolmogorov A N 1941 Dissipation of energy in the locally isotropic turbulence *Dokl. Akad. SSSR* **32** 19–21
[3] Marati N, Casciola C M and Piva R 2004 Energy cascade and spatial fluxes in wall turbulence *J. Fluid Mech.* **521** 191–215
[4] Cimarelli A, De Angelis E and Casciola C M 2013 Paths of energy in turbulent channel flows *J. Fluid Mech.* **715** 436–451
[5] Cimarelli A, De Angelis E and Casciola C M 2011 Assessment of the turbulent energy paths from the origin to dissipation in wall-turbulence *J. Phys.: Conf. Series* **318** 022007
[6] Smits A J, McKeon B J and Marusic I 2011 High Reynolds-number wall turbulence *Annu. Rev. Fluid Mech.* **43** 353–375
[7] Del Álamo J C, Jiménez J, Zandonade P and Moser R D 2006 Self-similar vortex clusters in the turbulent logarithmic region *J. Fluid Mech.* **561** 329–358
[8] Lozano-Durán A, Flores O and Jiménez J 2012 The three-dimensional structure of momentum transfer in turbulent channels *J. Fluid Mech.* **694** 100–130
[9] Jiménez J 1999 The physics of wall turbulence *Physica A* **263** 252–256
[10] Jiménez J 2012 Cascades in wall-bounded turbulence *Annu. Rev. Fluid Mech.* **44** 27–45
[11] Perry A E, Henbest S and Chong M S 1986 A theoretical and experimental study of wall turbulence *J. Fluid Mech.* **165** 163–199
[12] Cimarelli A 2011 *Statistical Analysis and Simulation Techniques in Wall-Bounded Turbulence* (PhD thesis, University of Bologna)
[13] Hill R J 2002 Exact second-order structure-function relationships *J. Fluid Mech.* **468** 317–326
[14] Segalini A, Cimarelli A, Ruedi J D, De Angelis E and Talamelli A 2011 Effect of the spatial filtering and alignment error of hot-wire probes in a wall-bounded turbulent flow *Meas. Sci. Technol.* **22** 105408
[15] Mizuno Y and Jiménez J 2013 Wall turbulence without walls *J. Fluid Mech.* **723** 429–455
[16] Hutchins N and Marusic I 2007 Large-scale influences in near-wall turbulence *Phil. Trans. R.Soc. A* **365** 647–664
[17] Jiménez J and Hoyas S 2008 Turbulent fluctuations above the buffer layer of wall-bounded flows *J. Fluid Mech.* **611** 215–236
[18] Monty J P, Stewart J A, Williams R C and Chong M S 2007 Large-scale features of turbulent pipe and channel flows *J. Fluid Mech.* **589** 147–156
[19] Bailey S C C and Smits A J 2010 Experimental investigation of the structure of large- and very-large-scale motions in turbulent pipe flow *J. Fluid Mech.* **651** 339–356
[20] Del Álamo J C and Jiménez J 2003 Spectra of the very large anisotropic scales in turbulent channels *Phys. Fluids* **15**, 6 41–44
[21] Cimarelli A and De Angelis E 2011 Analysis of the Kolmogorov equation for filtered wall-turbulent flows *J. Fluid Mech.* **676** 376–395
[22] Cimarelli A and De Angelis E 2012 Anisotropic dynamics and sub-grid energy transfer in wall-turbulence *Phys. Fluids* **24** 015102
[23] Piomelli U and Balaras E 2002 Wall-layer models for large-eddy simulations *Annu. Rev. Fluid Mech.* **34** 349–374
[24] Flores O and Jiménez J 2006 Effect of wall-boundary disturbances on turbulent channel flows *J. Fluid Mech.* **566** 357–376